

# Soft-x-ray emission, plasma equilibrium, and fluctuation studies on Madison Symmetric Torus

C. Xiao

*Department of Physics, University of Wisconsin-Madison, Madison, Wisconsin and Department of Physics and Engineering Physics, University of Saskatchewan, Saskatoon, Canada*

P. Franz

*Consorzio RFX-Associazione EURATOM ENEA Sulla Fusione, Italy and Istituto Nazionale di Fisica della Materia, Unita' di Ricerca di Padova, Italy*

B. E. Chapman and D. Craig

*Department of Physics, University of Wisconsin-Madison, Madison, Wisconsin*

W. X. Ding

*Department of Electrical Engineering, University of California, Los Angeles, California*

G. Gadani and L. Marrelli

*Consorzio RFX-Associazione EURATOM ENEA Sulla Fusione, Italy*

P. Martin

*Consorzio RFX-Associazione EURATOM ENEA Sulla Fusione, Italy and Istituto Nazionale di Fisica della Materia, Unita' di Ricerca di Padova, Italy*

R. Pasqualotto and G. Spizzo

*Consorzio RFX-Associazione EURATOM ENEA Sulla Fusione, Italy*

J. S. Sarff

*Department of Physics, University of Wisconsin-Madison, Madison, Wisconsin*

S. D. Terry

*Department of Electrical Engineering, University of California, Los Angeles, California*

(Presented on 11 July 2002)

A miniature multichord soft-x-ray detection system has been installed on the Madison Symmetric Torus (MST) reversed-field pinch to study the plasma equilibrium and fluctuation properties of standard- and improved-confinement discharges. Because of the relatively flat MST density and temperature profiles, the spatial resolution is relatively poor along the line of sight. However, the system can resolve line-integrated-emissivity fluctuations which are strongly correlated with the rotating  $m=1$  global magnetic fluctuations as well as heat pulse propagation with edge-resonant  $m=0$  bursts during improved-confinement discharges. Abel inversion based on Park's inversion techniques indicates peaking of the equilibrium emissivity profile following sawtooth events during standard discharges and profile flattening after  $m=0$  bursts during improved-confinement discharges. © 2003 American Institute of Physics. [DOI: 10.1063/1.1537875]

## I. INTRODUCTION

MHD activity associated with  $m=1$  and  $m=0$  fluctuations in a reversed-field pinch (RFP) is influenced by pressure and current-density profiles. The MHD phenomena in an RFP are also responsible for driving poloidal current, inducing a reversed toroidal magnetic field and leading the system to relax to a minimum-energy stable state. The MHD activity is also accompanied by increased particle and energy transport. In the Madison Symmetric Torus (MST) reversed-field pinch (major radius  $R=1.5$  m, minor radius  $a=0.52$  m),<sup>1</sup> efforts have been made to tailor the parallel current profile with inductive auxiliary current drive. Pulsed parallel current drive (PPCD)<sup>2</sup> inductively modifies the current profile, suppresses sawtooth crashes, reduces magnetic fluctuations, and significantly improves the energy confinement in MST.<sup>3</sup>

It is important to measure equilibrium and fluctuating profiles to gain insight into the physics underlying many important issues in a RFP, such as MHD instabilities and their effect on the energy confinement. As a new addition to the various diagnostic tools employed on the MST, a soft-x-ray (SXR) tomography system has recently been developed at Consorzio RFX to obtain the SXR emission profiles in the MST plasma. The initial operation of a single fan array has successfully provided MHD properties associated with  $m=1$  oscillations, sawtooth events during standard-confinement discharges, and  $m=0$  bursts during PPCD discharges.

We describe the SXR detection array used on MST in Sec. II. Then, we present some experimental results in Sec. III, concentrating on the features of the SXR signals associated with MHD activity. In Sec. IV we provide some concluding discussion.

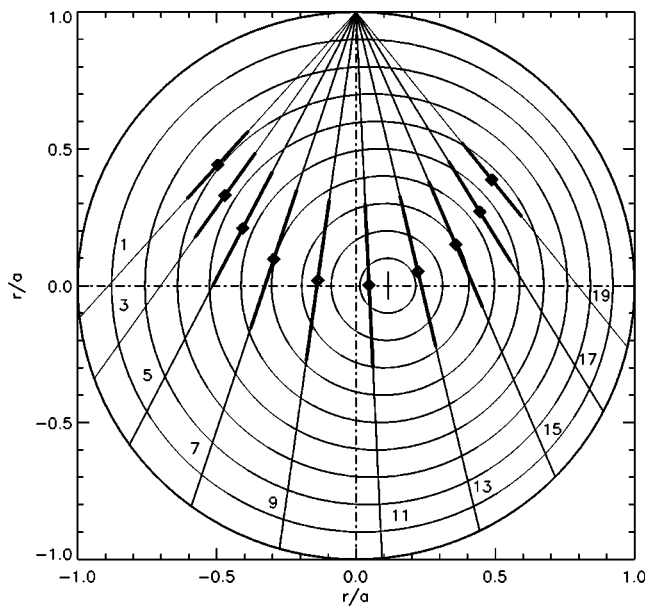


FIG. 1. Lines of sight of the SXR detector array in the MST reversed-field pinch. The diamonds indicate the centers of the lines of sight. The thick lines depict the regions that contribute 50% of the brightness for a simulated profile.

## II. SXR DETECTOR ARRAY

The SXR detection camera, designed and fabricated by the INFM-RFX Group within the framework of the INFM-PAIS Project “SOFTCAM,” consists of an IRD AXUV-20EL<sup>4</sup> diode array with 20 diodes, a pinhole image slit, and a beryllium filter of a chosen thickness (typically 16  $\mu\text{m}$ ). The miniature design allows the camera to be inserted through a small vertical port on MST. The lines of sight form a fan array. The plasma sampled by each diode has a radial spread of  $\sim 5$  cm at the midplane of MST and a toroidal spread of 41 cm. Therefore, half of each line of sight overlaps adjacent lines of sight. Utilizing only every other diode in the array, there is no overlap in the diode sampling volumes. We typically use 12 diodes in the array, covering most of the plasma cross section. Figure 1 shows the geometry of the fan array, using every other diode in the array, on a poloidal cross section. The Shafranov-shifted magnetic surfaces are also depicted.

The SXR emissivity depends on plasma electron density, temperature, and impurity concentration. In order to estimate the resolution along each line of sight, we have simulated bremsstrahlung radiation from a pure hydrogen plasma, the x-ray absorption of the beryllium filter, and the electron density, and temperature profiles. The density and temperature profiles are expressed in the following equations:

$$n = n_0 \left[ 1 - \left( \frac{r}{a} \right)^8 \right], \quad T_e = T_{e0} \left[ 1 - \left( \frac{r}{a} \right)^4 \right],$$

where  $r$  is the minor radial coordinate,  $a=0.52$  m is the minor radius of MST, and  $n_0=1 \times 10^{13} \text{ cm}^{-3}$  ( $T_{e0}=400$  eV) is the density (temperature) at  $r=0$ . In Fig. 1, the thick lines superimposed on the lines of sight represent the central portion of the line of sight that contributes 50% of the line-integrated emissivity. The simulations have also shown that

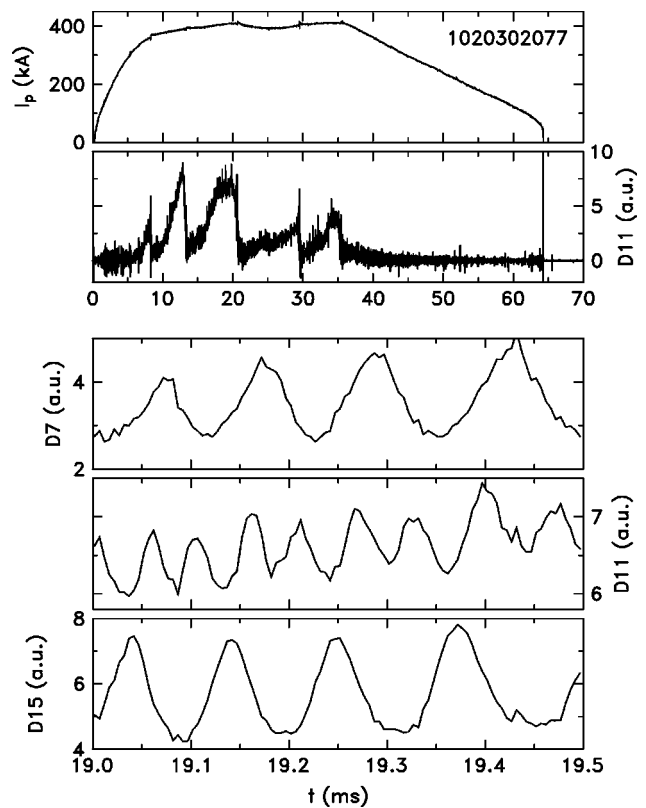


FIG. 2. Discharge current and SXR signals from different SXR diodes during a 400 kA standard discharge (shot No.: 1 020 302 077); refer to Fig. 1 for diode chords.

the localization of the SXR measurements is better if more peaked density and temperature profiles are assumed for the same camera configuration. Although the measured SXR signals are by no means localized, the signals are heavily weighted towards the high-plasma-thermal-pressure region. This allows identification of some long wavelength global plasma structures associated with MHD activity using only one array without performing inversion. An irregular emission structure in the plasma with a radial/poloidal extent even smaller than the thick lines in Fig. 1 may be identified since 10% variations in the brightness (line-integrated emissivity) signal can be easily distinguished.

## III. EXPERIMENTAL RESULTS

In this section we will describe the features of the SXR signals and their possible relation to MHD activity.

### A. Brightness fluctuations

Figure 2 depicts waveforms of plasma current and SXR signals during a standard-confinement 400 kA discharge in MST. Traces are (from top): plasma current  $I_p$ , SXR signal of diode 11, D11, near the Shafranov-shifted plasma center (see also Fig. 1), and three expanded SXR signals D7, D11, and D15 for diodes 7, 11, and 15, respectively, to emphasize the fluctuating part of the signals. During the discharge, the SXR signal D11 shows sawtooth features: it decreases sharply, recovers slowly, and decreases sharply again. All the other SXR diodes signals exhibit the same behavior. The sawtooth crash corresponds to magnetic reconnection. The

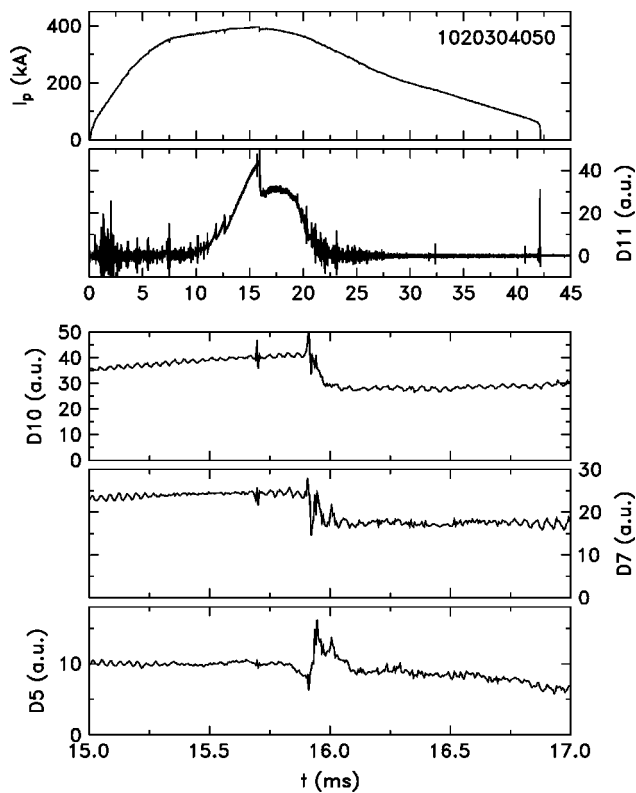


FIG. 3. Discharge current and SXR signals during a 400 kA PPCD discharge (shot No.: 1 020 304 050); refer to Fig. 1 for diode chords.

sudden drop in the SXR brightness at the sawtooth crash is an indicator of the confinement degradation, which has been measured with other diagnostics.

The expanded traces of D7 and D15, with centers of their lines of sight on the two sides of the Shafranov shifted centers, show nearly sinusoidal oscillations with  $\sim 180^\circ$  phase shift. The oscillation frequency is around 10 kHz. The signal of diode 11 near the shifted plasma center oscillates at twice the frequency of the off-center channels. This frequency doubling results from the rotation of a bright, off-center, helical structure.<sup>5,6</sup> These oscillations are highly coherent, at the fundamental frequency (10 kHz in this case), with the magnetic fluctuations detected by pickup coils at the plasma boundary, indicating that the magnetic fluctuations are closely related to the plasma temperature and density.

### B. Heat pulse propagation

Figure 3 shows the waveforms from a 400 kA PPCD discharge. The expanded traces for SXR signals D10, D7, and D5 are low-pass filtered (0.3 kHz) to emphasize the overall signal change after the  $m=0$  burst at  $t=15.8$  ms. The maximum SXR signal for D11 for this discharge is four times larger than that of the discharge shown in Fig. 2, indicating significantly higher electron temperature (constant density is controlled by gas puffing).

Unlike the standard-plasma sawtooth events during which the SXR brightness decreases by more than 80% percent, the decrease of the SXR signal is only 30% for the  $m=0$  burst in the PPCD discharge shown in Fig. 3, suggesting that perhaps some plasma region still maintains relatively

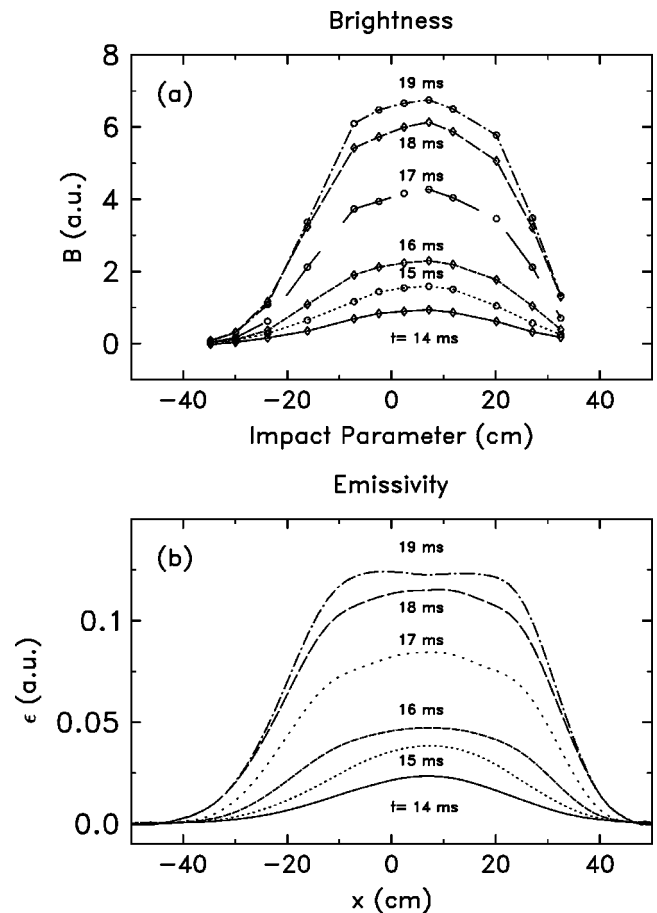


FIG. 4. (a) Line-integrated and (b) inverted SXR emission profiles at different times in a standard-confinement discharge (shot No.: 1 020 302 077). A sawtooth crash occurs just before 14 ms.

good confinement after the burst. The brightness of the in-board edge diode channels 1, 3, and 5 increases, and the brightness of other diode channels decreases after the burst. The time at which the maximum brightness occurs increases progressively for D5, D3, and D1, indicating radially outward heat pulse propagation. This phenomenon is similar to the sawtooth oscillations observed in the tokamak core region and the inverted oscillations in the edge region. Using a heat pulse propagation model developed for tokamaks,<sup>7</sup> the electron thermal diffusion coefficient during the  $m=0$  burst is roughly  $100 \text{ m}^2/\text{s}$  in the region  $r \sim 30 \text{ cm}$ .

### C. Equilibrium emissivity profiles

Abel inversion based on Parker's method<sup>8</sup> is used to obtain SXR emissivity profiles. Parker's method includes the Shafranov shift, assumes up-down symmetry, and can be applied to parallel vertical chords only. In our inversion algorithm, the fan array geometry has been included. Instead of assuming up-down symmetry, the total path length of the line of sight, which twice enters a zone between two dividing circles, is included in the equation set  $B_i = \sum L_{ij} \epsilon_j$ , where  $B_i$  is the brightness detected by diode  $i$ ,  $L_{ij}$  is the total path length in zone  $j$  for diode  $i$ , and  $\epsilon_j$  is the average emissivity at those two locations where the line of sight enters the zone  $j$ . Inversion applied to a set of simulated data based on a

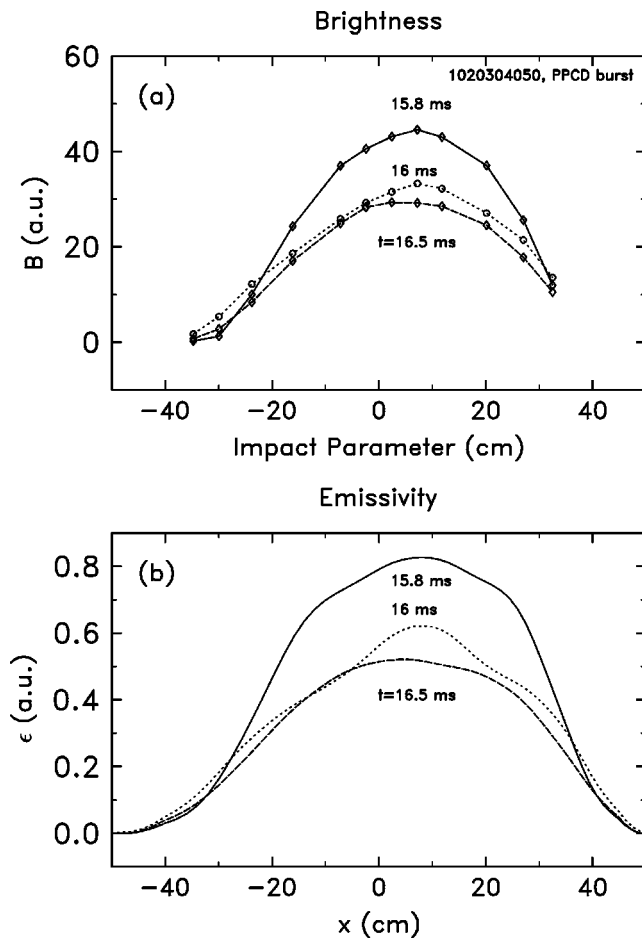


FIG. 5. (a) Line-integrated and (b) inverted SXR emission profiles before ( $t=15.8$  ms), during ( $t=16$  ms) and after ( $t=16.5$  ms) an  $m=0$  burst during a PPCD discharge (shot No.: 1 020 304 050).

known emissivity profile with a Shafranov shift recovers the assumed profiles and Shafranov shift value.

Figure 4 shows the time evolution of the brightness and inverted emissivity profiles for the 400 kA standard discharge shown in Fig. 2 during a sawtooth recovery phase from 14 to 19 ms. The  $m=1$  oscillations were filtered out

before the inversion. The emissivity profile is low and peaked at  $t=14$  ms immediately following the sawtooth crash and progressively increases and flattens between  $t=14$  ms and  $t=18$  ms. Finally, the profile becomes weakly hollow at  $t=19$  ms, before the next sawtooth crash. Figure 5 shows the brightness and inverted emissivity profiles for the PPCD discharge shown in Fig. 3. In contrast to the profile peaking after the sawtooth crash, the profile flattens after an  $m=0$  burst.

#### IV. CONCLUSIONS

The newly installed SXR detector array has been routinely used to monitor SXR radiation from the MST reversed-field pinch. Preliminary data analyses based on single shots have shown that the system is able to extract MHD-related SXR emission changes over the entire plasma. Despite its limited radial/poloidal resolution, the SXR detection system is capable of resolving features related to  $m=0$  and  $m=1$  MHD activity. To better reconstruct the emissivity structure associated with the  $m=1$  modes in MST, an additional diode array has been installed at the same toroidal location to view the plasma from a port with a poloidal offset of  $90^\circ$  with respect to the existing array.

#### ACKNOWLEDGMENTS

This work has been supported by the U.S. Department of Energy and NSERC Canada. The SXR diagnostic system has been developed within the framework of the INFM-PAIS Project "SOFTCAM." Support provided by the MST Group is appreciated with much gratitude.

<sup>1</sup>R. N. Dexter, D. W. Kerst, T. W. Lovell, S. C. Prager, and J. C. Spratt, *Fusion Technol.* **19**, 131 (1991).

<sup>2</sup>J. S. Sarff, S. A. Hokin, H. Ji, S. C. Prager, and C. R. Sovinec, *Phys. Rev. Lett.* **72**, 3670 (1994).

<sup>3</sup>B. E. Chapman *et al.*, *Phys. Rev. Lett.* **87**, 205001 (2001).

<sup>4</sup><http://www.ird-inc.com/axuvarr.html>

<sup>5</sup>G. Chartas and S. A. Hokin, *Phys. Fluids* **4**, 4019 (1992).

<sup>6</sup>P. Franz, G. Gadani, L. Marrel, P. Martin, R. Pasqualotto, B. Chapman, and C. Xiao, EPS 2002, paper p4.126, [http://elise.epfl.ch/pdf/P4\\_126.pdf](http://elise.epfl.ch/pdf/P4_126.pdf)

<sup>7</sup>J. D. Callen and G. L. Jahns, *Phys. Rev. Lett.* **38**, 491 (1977).

<sup>8</sup>H. K. Park, *Plasma Phys. Controlled Fusion* **31**, 2035 (1989).